

1 **Identification of novel bat coronaviruses sheds light on the**
2 **evolutionary origins of SARS-CoV-2 and related viruses**

3 Hong Zhou^{1,8}, Jingkai Ji^{1,8}, Xing Chen^{2,8}, Yuhai Bi^{3,8}, Juan Li¹, Tao Hu¹, Hao Song⁴,
4 Yanhua Chen², Mingxue Cui¹, Yanyan Zhang¹, Alice C. Hughes^{2,5,*}, Edward C.
5 Holmes^{6,*}, Weifeng Shi^{1,7,9,*}

6
7 ¹Key Laboratory of Etiology and Epidemiology of Emerging Infectious Diseases in
8 Universities of Shandong, Shandong First Medical University & Shandong Academy
9 of Medical Sciences, Taian 271000, China

10 ²Landscape Ecology Group, Center for Integrative Conservation, Xishuangbanna
11 Tropical Botanical Garden, Chinese Academy of Sciences, Menglun, Mengla, Yunnan
12 666303, China

13 ³CAS Key Laboratory of Pathogenic Microbiology and Immunology, Institute of
14 Microbiology, CAS Center for Influenza Research and Early-warning (CASCIRE),
15 CAS-TWAS Center of Excellence for Emerging Infectious Diseases (CEEID),
16 Chinese Academy of Sciences, Beijing 100101, China

17 ⁴Research Network of Immunity and Health (RNIH), Beijing Institutes of Life
18 Science, Chinese Academy of Sciences, Beijing 100101, China

19 ⁵Center of Conservation Biology, Core Botanical Gardens, Chinese Academy of
20 Sciences, Menglun, Mengla, Yunnan 666303, China

21 ⁶Marie Bashir Institute for Infectious Diseases and Biosecurity, School of Life and
22 Environmental Sciences and School of Medical Sciences, The University of Sydney,
23 Sydney, New South Wales 2006, Australia

24 ⁷Science and Technology Innovation Center, Shandong First Medical University &
25 Shandong Academy of Medical Sciences, Taian 271000, China

26 ⁸These authors contributed equally

27 ⁹Lead Contact

28 *Correspondence: shiwf@ioz.ac.cn (W.S.), edward.holmes@sydney.edu.au,

29 ach_conservation2@hotmail.com (A.C.H.)

30

31

32

33

34 **Summary**

35 Although a variety of SARS-CoV-2 related coronaviruses have been identified, the
36 evolutionary origins of this virus remain elusive. We describe a meta-transcriptomic
37 study of 411 samples collected from 23 bat species in a small (~1100 hectare) region
38 in Yunnan province, China, from May 2019 to November 2020. We identified
39 coronavirus contigs in 40 of 100 sequencing libraries, including seven representing
40 SARS-CoV-2-like contigs. From these data we obtained 24 full-length coronavirus
41 genomes, including four novel SARS-CoV-2 related and three SARS-CoV related
42 genomes. Of these viruses, RpYN06 exhibited 94.5% sequence identity to SARS-
43 CoV-2 across the whole genome and was the closest relative of SARS-CoV-2 in the
44 ORF1ab, ORF7a, ORF8, N, and ORF10 genes. The other three SARS-CoV-2 related
45 coronaviruses were nearly identical in sequence and clustered closely with a virus
46 previously identified in pangolins from Guangxi, China, although with a genetically
47 distinct spike gene sequence. We also identified 17 alphacoronavirus genomes,
48 including those closely related to swine acute diarrhea syndrome virus and porcine
49 epidemic diarrhea virus. Ecological modeling predicted the co-existence of up to 23
50 *Rhinolophus* bat species in Southeast Asia and southern China, with the largest
51 contiguous hotspots extending from South Lao and Vietnam to southern China. Our
52 study highlights both the remarkable diversity of bat viruses at the local scale and that
53 relatives of SARS-CoV-2 and SARS-CoV circulate in wildlife species in a broad
54 geographic region of Southeast Asia and southern China. These data will help guide
55 surveillance efforts to determine the origins of SARS-CoV-2 and other pathogenic
56 coronaviruses.

57 **Keywords**

58 SARS-CoV-2, COVID-19, coronavirus, evolution, bats, phylogeny, spike protein,
59 swine acute diarrhea syndrome, porcine epidemic diarrhea virus

60 **Introduction**

61 Most viral pathogens in humans have zoonotic origins, arising through occasional
62 (e.g. coronavirus, Ebola virus) or frequent (e.g. avian influenza A virus) animal
63 spillover infections. Bats (order Chiroptera) are the second most diverse mammalian
64 order after Rodentia and currently comprise ~1420 species, accounting for some 22%
65 of all named mammalian species (Letko et al., 2020). Bats are well known reservoir
66 hosts for a variety of viruses that cause severe diseases in humans, and have been
67 associated with the spillovers of Hendra virus, Marburg virus, Ebola virus and, most
68 notably, coronaviruses. Aside from bats and humans, coronaviruses can infect a wide
69 range of domestic and wild animals, including pigs, cattle, mice, cats, dogs, chickens,
70 deer and hedgehogs (Chan et al., 2013; Su et al., 2016; Corman et al., 2018).

71 By 2019 there were six known human coronaviruses (HCoV): HCoV-229E, HCoV-
72 OC43, severe acute respiratory syndrome coronavirus (SARS-CoV), HCoV-NL63,
73 HCoV-HKU1, and Middle East respiratory coronavirus (MERS-CoV) (Su et al., 2016;
74 Forni et al., 2017). HCoV-229E, HCoV-NL63, SARS-CoV and MERS-CoV were
75 known to have zoonotic origins, with bats likely important reservoir hosts, although
76 sometimes emergence in humans followed transmission through so-called
77 “intermediate” hosts such as palm civets for SARS-CoV and dromedary camels for
78 MERS-CoV (Corman et al., 2018; Ye et al., 2020). Similarly, it has been proposed that
79 rodents may be the natural hosts of HCoV-OC43 and HCoV-HKU1, with cattle a
80 possible intermediate host for HCoV-OC43 (Corman et al., 2018; Ye et al., 2020).

81 In early 2020, a novel coronavirus, SARS-CoV-2, was identified as the causative
82 agent of a pneumonia outbreak in Wuhan, China, that eventually turned into a global
83 pandemic (Zhu et al., 2020; Lu et al., 2020; Wu et al., 2020a). A combination of
84 retrospective genome sequencing and ongoing sampling then identified a number of
85 SARS-CoV-2 related coronaviruses in wildlife. These included: (i) the bat
86 (*Rhinolophus affinis*) virus RaTG13 that is the closest relative of SARS-CoV-2 across

87 the viral genome as a whole (Zhou et al., 2020b); (ii) the bat (*R. malayanus*) derived
88 coronavirus RmYN02 that is the closest relative of SARS-CoV-2 in the long ORF1ab
89 gene and which contains a similar nucleotide insertion at the S1/S2 cleavage site of
90 the spike gene (Zhou H et al., 2020a); (iii) viruses from the Malayan pangolin (*Manis*
91 *javanica*) that comprised two lineages reflecting their Chinese province of collection
92 by local customs authorities (Guangdong and Guangxi), with the pangolins from
93 Guangdong possessing identical amino acids at the six critical residues of the receptor
94 binding domain (RBD) to human SARS-CoV-2 (Lam et al., 2020; Xiao et al., 2020);
95 and (iv) a more distant SARS-CoV-2 related coronavirus from a bat (*R. cornutus*)
96 sampled in Japan (Murakami et al., 2020). More recently, two novel
97 betacoronaviruses (STT182 and STT200) were described in *R. shameli* bats sampled
98 from Cambodia in 2010 that share 92.6% nucleotide identity with SARS-CoV-2 as
99 well as five of the six critical RBD sites observed in SARS-CoV-2 (Hul et al., 2021).
100 In addition, a novel bat (*R. acuminatus*) coronavirus isolated from Thailand
101 (RacCS203) in June 2020 was recently identified and found to be closely related to
102 RmYN02 (Wacharapluesadee et al., 2021). Collectively, these studies indicate that
103 bats across a broad swathe of Asia harbor coronaviruses that are closely related to
104 SARS-CoV-2 and that the phylogenetic and genomic diversity of these viruses has
105 likely been underestimated. Herein, we report the discovery of additional bat
106 coronaviruses from Yunnan province, China that reveal more of the diversity and
107 complex evolutionary history of these viruses, including both cross-species
108 transmission and genomic recombination.

109 **Results**

110 **Identification of novel bat coronaviruses**

111 From May 2019 to November 2020, a total of 283 fecal samples, 109 oral swabs and
112 19 urine samples were collected from bats in Yunnan province, China. The majority of
113 samples were collected from horseshoe bats, comprising: *Rhinolophus malayanus*

114 (n=88), *R. stheno* (n=36), *R. sinicus* (n=34), and *R. siamensis* (n=12), *R. pusillus*
115 (n=2), other *Rhinolophus* sp. (n=11), and *Hipposideros larvatus* (n=59) (Figure 1A
116 and 1B, Table S1). These samples were pooled into 100 libraries (numbered p1 to
117 p100) according to the collection date and host species, with each library containing
118 one to 11 samples. Meta-transcriptomic (i.e. total RNA) sequencing was performed
119 and coronaviruses contigs were identified in 40 libraries (Table S2). Blastn searches
120 of the *de novo* assemblies identified 26 long contigs (>23,000 nt in length) that
121 mapped to coronavirus genomes present in 20 libraries, including nine sarbecoviruses
122 (i.e. from the genus *Betacoronavirus*) and 17 alphacoronaviruses. The number of
123 read-pairs mapping to these long contigs ranged from 3,433 to 21,498,614, with the
124 average depth ranging from 35.86 to 215,065.00 (Table S3). It should be noted that
125 pool p1 comprising 11 fecal samples from *R. malayanus* was the same pool
126 previously used to identify RmYN01 and RmYN02 (Zhou et al., 2020a). The
127 remaining 24 genomes were named in the same manner, in which the first two letters
128 represent an abbreviation of the bat species, YN denotes Yunnan, and the final number
129 is a serial number ranging from 03 to 26. In addition, several short contigs related to
130 SARS-CoV-2 were identified in two other libraries - p7 and p11 (Figure S1, Table
131 S2).

132 Further Blastn analyses revealed that four of the seven novel sarbecoviruses identified
133 here (RpYN06, RsYN04, RmYN05, and RmYN08) were related to SARS-CoV-2
134 with nucleotide identities ranging from 82.46% to 97.21%, while the remaining three
135 (RsYN03, RmYN07, and RsYN09) were more closely related to SARS-CoV with
136 nucleotide identities ranging from 91.60% to 93.28%. We next designed specific
137 primers and a probe set of quantitative real-time PCR primers (qPCR) (Table S4) that
138 targeted the conserved region of the 1a gene region to detect the presence of the four
139 SARS-CoV-2 related viruses in individual bats (i.e. prior to sample pooling; Figure
140 1C). Pool p46 only contained only a single positive fecal sample, no. 379, collected
141 on May 25, 2020, and the virus was detected with a cycle threshold (*Ct*) value of
142 26.97 (Figure 1C). SARS-CoV-2 related virus was also detected in three (sample nos.

143 362, 364, and 372) of the six, three (sample nos. 367, 391, and 397) of the eight, and
144 two (sample nos. 448 and 450) of the seven samples in pool nos. p35, 44 and 62,
145 respectively, with *Ct* values ranging from 26.10 to 32.82 (Figure 1C). Among these,
146 samples 362, 364, 372 and 367 were collected on May 25, 2020, 391 and 397 were
147 collected on June 3, 2020, while both 448 and 450 were collected on July 16, 2020.
148 The 5' and 3' termini and the spike gene sequences of the four coronaviruses related
149 to SARS-CoV-2 were verified using individual samples 379, 364, 367 and 450 with 5'
150 and 3' RACE (Table S4) and Sanger sequencing. Results from Sanger sequencing
151 were consistent with those obtained from the meta-transcriptomic sequencing.

152 **Sequence identities between SARS-CoV-2 and related viruses**

153 At the scale of the whole genome, RpYN06 exhibited 94.5% sequence identity to
154 SARS-CoV-2, making it, after RaTG13 (96.0%), the second closest relative of SARS-
155 CoV-2 documented to date (Figure 2). However, because of extensive recombination,
156 patterns of sequence similarity vary markedly across the virus genome, and RmYN02
157 shared 97.18% sequence identity with SARS-CoV-2 in the 1ab open reading frame
158 (ORF), compared to 97.19% for RpYN06. In addition to the ORF1ab, RpYN06
159 shared the highest nucleotide identities with SARS-CoV-2 in the RdRp (RNA-
160 dependent RNA polymerase; 98.36%), ORF7a (96.72%), ORF8 (97.54%), N
161 (97.70%), and ORF10 (100%) (Figure 2, Table S5 and S6). However, RpYN06
162 exhibited only 76.3% nucleotide identity to the SARS-CoV-2 spike gene and 60.9% in
163 the receptor binding domain (RBD), thereby similar to RmYN02, ZC45, ZXC21 and
164 the Thailand coronavirus strains (Figure 2). Excluding the spike gene, the sequence
165 identities of RpYN06, RmYN02 and RaTG13 to SARS-CoV-2 were 97.17%, 96.41%
166 and 96.49%, respectively.

167 In contrast, RsYN04, RmYN05 and RmYN08 exhibited >99.96% nucleotide
168 identities to each other at the scale of the whole genome. Such strong similarity is
169 indicative of viruses from the same species, even though they were sequenced on

170 different lanes and the samples were collected from different bat species at different
171 time points. In addition, they shared low nucleotide identities with SARS-CoV-2
172 across the whole genome (76.5%), particularly in the spike gene, ORF3a, ORF6,
173 ORF7a, ORF7b and ORF8 with nucleotide identities <70% (Figure 2). Interestingly,
174 when using RsYN04 as the query sequence, the closest hit in the Blastn search was
175 the pangolin derived coronavirus MP789 (MT121216.1) with 82.9% nucleotide
176 identity.

177 **Evolutionary history of sarbecoviruses**

178 Phylogenetic analysis of full-length genome sequences of representative
179 sarbecoviruses revealed that SARS-CoV-2 was most closely related to RaTG13, while
180 RmYN02 and the Thailand strains formed a slightly more divergent clade. Notably,
181 RpYN06 was placed at the basal position of the clade containing SARS-CoV-2 and its
182 closest relatives from bats and pangolins (Figure 3A, Table S6). In contrast, RsYN04,
183 RmYN05 and RmYN08 grouped together and clustered with the pangolin derived
184 viruses from Guangxi, although being separated from them by a relatively long
185 branch. Finally, three SARS-CoV related coronaviruses (RsYN03, RmYN07, and
186 RsYN09) fell within the SARS-CoV lineage, grouping with other bat viruses
187 previously sampled in Yunnan (Figure 3A).

188 A different topological pattern was observed in the phylogeny of the RdRp (Figure
189 3B). In particular, RpYN06 now grouped with RmYN02 (although with weak
190 bootstrap support), with together formed a clade with RaTG13, the two Cambodian
191 strains, and SARS-CoV-2 (Figure 3B). The two bat derived strains from Thailand
192 formed a separate lineage. Perhaps more striking was that RsYN04, RmYN05 and
193 RmYN08 now grouped with the Guangdong pangolin viruses (rather than those from
194 Guangxi; Figure 3B). A different pattern again was observed in the phylogeny of the
195 entire ORF1ab (Figure 3C). RpYN06 and RmYN02 now formed a clade and that was
196 the direct sister-group to SARS-CoV-2, with RaTG13 a little more divergent (Figure

197 3C). In addition, RsYN04, RmYN05 and RmYN08 now clustered with the pangolin
198 derived strains from Guangxi (Figure 3C), consistent with the complete genome
199 phylogeny.

200 In the spike gene phylogeny, SARS-CoV-2 and RaTG13 still grouped together, with
201 both pangolin lineages falling as sister groups (Figure 3D). The two Cambodian bat
202 viruses formed a separate and more divergent lineage. Strikingly, RpYN06 exhibited
203 marked phylogenetic movement, this time clustering with two previously described
204 bat viruses from Zhejiang province - ZC45 and ZXC21 - whereas the Thailand bat
205 virus clustered closely with RmYN02 (Figure 3D). In addition, RsYN321B,
206 RmYN363B, and RmYN442B did not fall within the SARS-CoV and SARS-CoV-2
207 clades, but instead formed a separate and far more divergent lineage (Figure 3D).
208 Finally, in the phylogeny of the RBD region, SARS-CoV-2 clustered with the
209 pangolin viruses from Guangdong with the two Cambodian bat viruses the next most
210 closely related viruses (Figure S2). RpYN06 fell within a lineage comprising several
211 bat derived betacoronaviruses, including ZC45, ZXC21, RsYN09, RsYN03, and
212 RmYN07. As expected given the complete S gene tree, bat viruses RsYN04,
213 RmYN05 and RmYN08 grouped together and formed a lineage, characterized by a
214 long branch (Figure S2).

215 **Molecular characterizations of the spike protein of the novel bat** 216 **sarbecoviruses**

217 At the six amino acid positions deemed critical for binding to the human angiotensin-
218 converting enzyme 2 (hACE2) receptor, SARS-CoV-2 and the three bat derived
219 viruses identified here (RsYN04, RmYN05 and RmYN08) shared L455 and Y505. In
220 contrast, despite being a closer overall relative, RpYN06 only possessed one identical
221 amino acid with SARS-CoV-2 - Y505 (Figure 4A). In the S1/S2 cleavage site of the
222 spike gene, none of the four SARS-CoV-2 related viruses reported here possessed a
223 similar insertion/deletion (indel) pattern as SARS-CoV-2 (Garry et al., 2021) (Figure

224 4A). Interestingly, however, the recently sampled bat virus from Thailand possessed a
225 PVA three amino acid insertion at this site, similar to the PAA insertion found in
226 RmYN02. In addition, two indel events have been identified in the RBD of many bat
227 associated coronaviruses (Holmes et al., 2021), including RpYN06 that was
228 characterized by indel patterns identical to those of ZC45 and ZXC21 (Figure 4A).
229 There were no indel events in SARS-CoV-2 and the pangolin derived coronaviruses in
230 RBD, and RsYN04, RmYN05 and RmYN08 possessed one unique indel event
231 different from other sarbecoviruses (Figure 4A). In addition, and similar to other bat
232 derived coronaviruses, the four novel SARS-CoV-2 related viruses possessed several
233 indel events in the N-terminal domain, while RsYN04, RmYN05 and RmYN08 again
234 possessed a unique indel pattern (Figure S3). Notably, RpYN06, ZC45, ZXC21 and
235 the Guangdong pangolin virus shared the same indel pattern, with RpYN06 exhibiting
236 high amino acid identity to these viruses in the N-terminal domain (amino acid
237 identities ranging from 85.3% to 99.0%; Figure S4).

238 We predicted and compared the three-dimensional structures of RpYN06, RsYN04
239 and SARS-CoV-2 using homology modeling (Figures 4B-4D). In a similar manner to
240 RmYN02 (Zhou et al., 2020a), the RBD of RpYN06 had two shorter loops than those
241 observed in SARS-CoV-2, while RsYN04 only had one shorter loop (Figure 4D). In
242 addition, near the S1/S2 cleavage sites, the conformational loop of RpYN06 and
243 RsYN04 were different from those of SARS-CoV-2 (Figures 4B-4C). Notably,
244 RsYN04 exhibited greater amino acid identity (71.28%) and shared more structural
245 similarity with the SARS-CoV-2 RBD than RpYN06 (63.08%). Importantly, the
246 conformational variations caused by these amino acid substitutions and deletions were
247 speculated to interfere with the binding of RpYN06 and RsYN04 RBD to hACE2
248 (Figure 4D). However, RsYN04 exhibited lower structural similarity with SARS-
249 CoV-2 in the N-terminal domain (NTD) (Figure 4C, black arrowheads, 39.19% amino
250 acid identity) than RpYN06 (65.87% amino acid identity).

251 **Phylogenetic analysis of the novel bat alphacoronaviruses**

252 As well as betacoronaviruses, we identified 17 novel bat alphacoronaviruses.
253 Phylogenetic analyses of the full-length genomes (Figure 5A), the RdRp genes
254 (Figure 5B), and ORF1ab (Figure S5) of these 17 alphacoronaviruses and
255 representative background viruses were consistent, with all trees revealing that the
256 viruses newly identified here fell within four established subgenera: *Decacovirus*
257 (n=12), *Pedacovirus* (n=1), *Myotacovirus* (n=1), and *Rhinacovirus* (n=2) (Figure 5).
258 Of particular note were MIYN15 and RsYN25 isolated from *Myotis laniger* and *R.*
259 *stheno* bats that were closely related to swine acute diarrhea syndrome coronavirus
260 (SADS-CoV) (Figure 5) (Zhou et al., 2018) sharing nucleotide identities 87.55% -
261 87.61%. In addition, HIYN18, isolated from a *Hipposideros larvatus* bat, fell within
262 the subgenus *Pedacovirus*, and was close to the porcine epidemic diarrhea virus
263 (PEDV) lineage (Figure 5). Notably, the virus CpYN11 (isolated from *Chaerephon*
264 *plicatus*) clustered with WA3607 (GenBank accession no. MK472070; isolated from a
265 bat from Australia), which together might represent an unclassified subgenus (Figure
266 5). Finally, RsYN14, RmYN17, McYN19, and RmYN24, although isolated from
267 different bat species and sequenced on different lanes, they were almost identical
268 (with nucleotide identity >99.98% to each other) and might represent a novel species
269 of subgenus *Decacovirus*.

270 Although the phylogenetic trees of the spike gene (Figure S6A) and protein sequences
271 (Figure S6B) were topologically similar to those of the full-length genome, RdRp and
272 ORF1ab, a number of notable differences were apparent indicative of past
273 recombination events. First, CpYN11 clustered with HKU8 rather than WA3607 in
274 the spike gene tree where they formed a separate lineage. Second, the topology of the
275 subgenus *Decacovirus* in the spike gene tree was different to those observed in other
276 gene regions. Finally, the two viruses belonging to the subgenus *Tegacovirus* were
277 placed into the subgenera *Pedacovirus* (GenBank accession no. NC_028806) and a
278 separate lineage (GenBank accession no. DQ848678), respectively.

279 **Ecological modeling of the distribution of *Rhinolophus* species in Asia**

280 To better understand the ecology of bat coronaviruses, we modeled the distribution of
281 49 *Rhinolophus* species in Asia using the collated distribution data and several
282 ecological measures (Figures 6 and S7). The models performed well with a mean Area
283 Under Curve (AUC) of 0.96 for training and 0.92 for testing, and all training AUCs
284 were above 0.88. Continentality (reflecting the difference between continental and
285 marine climates) was, on average, the most important factor, contributing an average
286 of 14.91% (based on permutation importance), followed by temperature seasonality at
287 11.7% average contribution, mean diurnal temperature range at 5.69%, and annual
288 potential evapotranspiration at 5.38%. Three additional ecological factors also
289 contributed over 5% on average: minimum precipitation at 5.25%, potential
290 evapotranspiration seasonality at 5.17% and Emberger's pluviothermic quotient (a
291 measure of climate type) at 5%. The next most important factor was the distance to
292 bedrock (an indicator of potential caves and rock outcrops) at 4.46%. Thus, local
293 climate, especially factors that influence diet availability across the year, is seemingly
294 key to determining bat species distributions across the region.

295 Although we could not accurately model diversity for Indonesia because of limited
296 recently available data and likely high endemism, mainland Southeast Asia was well
297 mapped (Figures 6 and S7). Most of mainland Southeast Asia's remaining tropical
298 forests showed a high diversity of Rhinolophid bats, with a maximum of 23 species
299 estimated to exist concurrently (Figure 6A). Rhinolophid hotspots occurred in forests
300 throughout much of mainland Southeast Asia, with the largest contiguous hotspots
301 extending from South Lao and Vietnam to Southern China (Figure 6A). Hotspots
302 were also identified in the Hengduan mountains, and some parts of northern Myanmar
303 and Nagaland in India (Figure 6A).

304 Interestingly, *R. affinis* (Figure 6B) and *R. pusillus* (Figure 6C) were widely
305 distributed in Southeast Asia and southern China, and most bat species shared

306 hotspots in Cambodia and peninsula Thailand. Several Rhinolophid species extended
307 their ranges northwards into southern China reflecting the presence of forest (*R.*
308 *affinis* and *R. pusillus*), whereas the geographic range of *R. malayanus* only just
309 reached southern China (Figures 6D-6F). Ecological drivers for these species
310 unsurprisingly showed some differences. Specifically, *R. affinis* was also influenced
311 by temperature seasonality (16.59%), followed by Emberger's pluviothermic quotient
312 and mean diurnal range (8.79, and 8.7%), while *R. malayanus* (a smaller species) was
313 mainly influenced by annual potential evapotranspiration mean (33.79%) and
314 seasonality (14.57%). *R. pusillus* was influenced by temperature seasonality (12.44%)
315 and continentality (9%), and *R. shameli* was largely influenced by annual potential
316 evapotranspiration seasonality (34.81%) followed by annual evapotranspiration
317 (9.79%). Overall, these factors control the range limits, and food availability for these
318 bat species.

319 It should be noted that the ecological modeling identified several other Rhinolophid
320 species with wide geographic distributions: *R. huanensis*, *R. lepidus*, *R. luctus*, *R.*
321 *macrotis*, *R. marshalli*, *R. microglobosus*, *R. pearsoni*, *R. rouxii*, *R. stheno*, *R.*
322 *thomasi*, and *R. yunnanensis* (Figure S7). Notably, *R. stheno* was found to host both
323 SARS-CoV-2 and SARS-CoV-like coronaviruses in the present study.

324 **Discussion**

325 To reveal more of the diversity, ecology and evolution of bat viruses, we collected bat
326 samples in Yunnan province, China during 2019-2020. Overall, 40 of the 100
327 sequencing libraries contained coronaviruses, including seven libraries with contigs
328 that could be mapped to SARS-CoV-2. In particular, we assembled 24 novel
329 coronavirus genomes from different bat species, including four SARS-CoV-2 like
330 coronaviruses. Further PCR based tests revealed that these four viruses tested positive
331 in nine individual samples collected in Yunnan province between May and July 2020.
332 Together with the SARS-CoV-2 related virus collected from Thailand in June 2020

333 (Wacharapluesadee et al., 2021), these results clearly demonstrate that SARS-CoV-2
334 related viruses continue to circulate in bat populations, and in some regions the
335 prevalence of SARS-CoV-2 related coronaviruses might be relatively high.

336 Of particular note was that one of the novel bat coronavirus identified here - RpYN06
337 - exhibited 94.5% sequence identity to SARS-CoV-2 across the genome as a whole
338 and in some individual gene regions (ORF1ab, ORF7a, ORF8, N, and ORF10) was
339 the closest relative of SARS-CoV-2 identified to date. However, the low sequence
340 identity in the spike gene, itself clearly the product of a past recombination event,
341 made it a second closest relative of SARS-CoV-2, next to RaTG13, at the genomic
342 scale. Hence, aside from the spike gene, RpYN06 possessed a genomic backbone that
343 is arguably the closest to SARS-CoV-2 identified to date.

344 Although several SARS-CoV-2-like viruses have been identified from different
345 wildlife species that display high sequence similarity to SARS-CoV-2 in some
346 genomic regions, none are highly similar (e.g. >95%) to SARS-CoV-2 in the spike
347 gene in terms of both the overall sequence identity and the amino acid residues at
348 critical receptor binding sites (Zhou et al., 2020b; Lam et al., 2020; Xiao et al., 2020;
349 Zhou et al., 2020a; Murakami et al., 2020; Hul et al., 2021; Wacharapluesadee et al.,
350 2021). Indeed, the spike protein sequences of three of the novel coronaviruses
351 described here (RsYN04, RmYN05, RmYN08) formed an independent lineage
352 separated from known sarbecoviruses by a relatively long branch. In this context it is
353 interesting that the recently identified bat coronavirus from Thailand carried by a
354 three-amino acid-insertion (PVA) at the S1/S2 cleavage site (Wacharapluesadee et al.,
355 2021). Although this motif is different to that seen in SARS-CoV-2 (PRRA) and
356 RmYN02 (PAA), this once again reveals the frequent occurrence of indel events in
357 the spike proteins of naturally sampled betacoronaviruses (Garry et al., 2021; Holmes
358 et al., 2021). Collectively, these results highlight the extremely high, and likely
359 underestimated, genetic diversity of the sarbecovirus spike proteins, and which likely
360 reflects their adaptive flexibility.

361 Previous studies have revealed frequent host switching of coronaviruses among bats
362 (Latinne et al., 2020). Indeed, we identified nearly 100% identical coronaviruses from
363 multiple different bat species both in *Alphacoronavirus* and *Betacoronavirus*,
364 indicative of the frequent cross-species virus transmission that drives virus evolution.
365 This in part likely reflects their roosting behavior and propensity to share the same or
366 close habitats. However, while facilitating host jumping, that individual bat species
367 can harbor multiple viruses increases the difficulty in resolving the origins of SARS-
368 CoV-2 and other pathogenic coronaviruses. Of particular note was that the three of the
369 newly identified SARS-CoV-2 like coronaviruses grouped together with the pangolin
370 derived coronaviruses from Guangxi in the whole genome phylogeny. Although the
371 associated branch lengths are relatively long such that other hosts may be involved,
372 and there are some topological differences between gene trees, this is suggestive of
373 virus transmission between pangolins and bats. Recently, a new SARS-CoV-2 related
374 coronavirus was identified from a pangolin from Yunnan (GISAID ID
375 EPI_ISL_610156). Whether pangolin derived coronaviruses have formed a separate
376 lineage clearly warrants further investigation.

377 Rhinolophid bats are important hosts for coronaviruses (Fan et al., 2019; Latinne et
378 al., 2020). Our ecological modeling revealed high richness of Rhinolophids across
379 much of Southeast Asia and southern China, with up to 23 species projected to co-
380 exist from the 49 species included in analysis. The largest expanses of high bat
381 diversity habitat stretch from South Vietnam into southern China (Hughes et al., 2012;
382 Allen et al., 2017). Indeed, it is striking that all the bat viruses described here, as well
383 as RmYN01 and RmYN02 described previously (Zhou et al., 2020a), were identified
384 in a small area (~1100 hectare) in Yunnan province. This highlights the remarkable
385 phylogenetic and genomic diversity of bat coronaviruses in a tiny geographic area and
386 to which humans may be routinely exposed. Importantly, in addition to Rhinolophids,
387 this broad geographic region in Asia is rich in many other bat families (Anthony et al.,
388 2017) and other wildlife species (Olival et al., 2017) that have been shown to be
389 susceptible to SARS-CoV-2 *in vitro* (Conceição et al., 2020; Wu et al., 2020; Sang et

390 al., 2020; Yan et al., 2021). It is therefore essential that further surveillance efforts
391 should cover a broader range of wild animals in this region to help track ongoing
392 spillovers of SARS-CoV-2, SARS-CoV and other pathogenic viruses from animals to
393 humans.

394 **Acknowledgments**

395 This work was supported by the Academic Promotion Programme of Shandong First
396 Medical University (2019QL006), the Key research and development project of
397 Shandong province (2020SFXGFY01 and 2020SFXGFY08), the National Science and
398 Technology Major Project (2020YFC0840800 and 2018ZX10101004-002), the
399 National Major Project for Control and Prevention of Infectious Disease in China
400 (2017ZX10104001-006), the Strategic Priority Research Programme of the Chinese
401 Academy of Sciences (XDB29010102 and XDA20050202), the Chinese National
402 Natural Science Foundation (32041010 and U1602265), and the High-End Foreign
403 Experts Program of Yunnan Province (Y9YN021B01). W.S. was supported by the
404 Taishan Scholars Programme of Shandong Province (ts201511056). Y.B. is supported
405 by the NSFC Outstanding Young Scholars (31822055) and Youth Innovation Promotion
406 Association of CAS (2017122). E.C.H. is supported by an ARC Australian Laureate
407 Fellowship (FL170100022). We thank all the scientists who kindly shared their
408 genomic sequences of the coronaviruses used in this study.

409 **Author Contributions**

410 W.S., E.C.H. and A.C.H. designed and supervised research. X.C., Y.C. and A.C.H.
411 collected the samples. H.Z., Y.B., M.C. and Y.Z. processed the samples. H.Z. performed
412 the 5' and 3' RACE, Sanger sequencing and molecular detection. J.J., J.L. and T.H.
413 performed the genome assembly and annotation. J.J., H.Z. and J.L. performed the
414 genome analysis and interpretation. J.L. and H.S. performed the homology modelling.
415 A.C.H. performed the ecological modeling. X.C. and Y.B. assisted in data interpretation

416 and edited the paper. W.S., E.C.H. and A.C.H. wrote the paper.

417 **Declaration of Competing Interests**

418 The authors declare no competing interests.

419 **Figure Legends**

420 **Figure 1. Sampling information and detection of SARS-CoV-2-like viruses in**
421 **individual bat fecal samples.**

422 (A) Sample numbers of different bat species captured live in Yunnan province from
423 May 2019 to November 2020. (B) Numbers of samples collected from different time
424 points (orange column - feces; green - oral swab; light purple - urine). The numbers of
425 individual bats are shown with black dots and relate to the y-axis. The associated
426 numbers are in the form sample numbers/number of individual bats. (C) Identification
427 of SARS-CoV-2-like virus positive samples using qPCR. Also see Tables S1 and S5.

428 **Figure 2. Sequence identities between SARS-CoV-2 and representative**
429 **sarbecoviruses.**

430 (A) Pairwise sequence identities between SARS-CoV-2 (reference genome:
431 NC_045512), and SARS-CoV-2 related coronaviruses. The degree of sequence
432 similarity is highlighted by the shading, with cells shaded red denoting the highest
433 identities. (B) Whole genome sequence similarity plot of nine SARS-CoV-2 related
434 coronaviruses using the SARS-CoV-2 as a query. The analysis was performed using
435 Simplot, with a window size of 1000bp and a step size of 100bp. Also see Tables S2
436 and S6.

437 **Figure 3. Phylogenetic analysis of SARS-CoV-2 and representative sarbecoviruses.**

438 Nucleotide sequence phylogenetic trees of (A) the full-length virus genome, (B) the
439 RdRp gene, (C) the ORF1ab, and (D) the spike gene. The phylogenetic trees in panels
440 A-C were rooted using the bat viruses Kenya_BtKY72 (KY352407) and
441 Bulgaria_BM48_31_BGR (GU190215) as outgroups, whereas the tree in panel D was

442 midpoint rooted for clarity only. Phylogenetic analysis was performed using RAxML
443 (Stamatakis 2014) with 1000 bootstrap replicates, employing the GTR nucleotide
444 substitution model. Branch lengths are scaled according to the number of nucleotide
445 substitutions per site. Viruses are color-coded as follows: red - SARS-CoV-2; blue -
446 new genomes generated in this study; green - recently published sequences from
447 Thailand and Cambodia. Also see Table S6.

448 **Figure 4. Molecular characterizations of the RBD and homology modeling of the**
449 **S1 subunit of the novel sarbecoviruses.**

450 (A) Sequence alignment of the RBD region of SARS-CoV-2 and representative
451 betacoronavirus genomes (annotation following Holmes et al., 2021). (B-C) Homology
452 modeling and structural comparison of the S1 subunit between (B) RpYN06 and SARS-
453 CoV-2, and (C) RsYN04 and SARS-CoV-2. (D) Structural similarity between the
454 RpYN06:hACE2, RsYN04:hACE2 and SARS-CoV-2-RBD:hACE2 complexes. The
455 three-dimensional structures of the S1 from RpYN06, RsYN04 and SARS-CoV-2 were
456 modeled using the Swiss-Model program (Waterhouse et al., 2018) employing PDB:
457 7A94.1 as the template. The S1 domains of RpYN06, RsYN04 and SARS-CoV-2 are
458 colored blue, orange and gray, respectively. The hACE2 are colored yellow. The
459 deletions in RpYN06 and/or RsYN04 are highlighted. The NTD (black arrow heads) is
460 marked. Also see Figure S3.

461 **Figure 5. Phylogenetic analysis of 17 novel alphacoronaviruses and representative**
462 **viruses from different subgenera.**

463 Phylogenetic trees of (A) the full-length virus genome and (B) the RdRp gene of
464 alphacoronaviruses. Phylogenetic analysis was performed using RAxML(Stamatakis
465 2014) with 1000 bootstrap replicates, employing the GTR nucleotide substitution
466 model. The two trees were rooted using two betacoronaviruses as outgroups -
467 South_Africa_PML-PHE1/RSA/2011 (KC869678.4) and HCoV-MERS-EMC
468 (NC_019843). Branch lengths are scaled according to the number of substitutions per
469 site. Also see Figures S4 and S8.

470 **Figure 6. Ecological modeling the geographical distribution of 49 Rhinolophid bat**
471 **species.**

472 (A) Models of 49 *Rhinolophus* bat species that predict diversity in five regions covering
473 mainland Southeast Asia, Philippines, Java-Sumatra, Borneo and Sulawesi-Moluccas.
474 The map color represents species richness, with up to 23 species projected to co-exist.
475 (B-F) Location distribution of (B) the RaTG13 host species *R. affinis*, (C) the RpYN06
476 host species *R. pusillus*, (D) the RmYN02 host species *R. malayanus*, (E) the RacCS203
477 host species *R. accuminatus*, and (F) the STT182 and STT200 host species *R. shameli*.
478 The yellow region represents the predicted range of each species. Also see Figure S7.
479

480 **References**

- 481 Allen, T., Murray, K.A., Zambrana-Torrel, C., Morse, S.S., Rondinini, C., Di Marco, M., Breit,
482 N., Olival, K.J., and Daszak, P. (2017). Global hotspots and correlates of emerging zoonotic diseases.
483 *Nat Commun* 8, 1124.
- 484 Anthony, S.J., Johnson, C.K., Greig, D.J., Kramer, S., Che, X., Wells, H., Hicks, A.L., Joly, D.O.,
485 Wolfe, N.D., Daszak, P., *et al.* (2017). Global patterns in coronavirus diversity. *Virus Evol* 3, vex012.
- 486 Camacho, C., Coulouris, G., Avagyan, V., Ma, N., Papadopoulos, J., Bealer, K., and Madden, T.L.
487 (2009). BLAST+: architecture and applications. *BMC Bioinformatics* 10, 421.
- 488 Chan, J.F., To, K.K., Tse, H., Jin, D.Y., and Yuen, K.Y. (2013). Interspecies transmission and
489 emergence of novel viruses: lessons from bats and birds. *Trends Microbiol* 21, 544-555.
- 490 Chen, J., Zhao, Y., and Sun, Y. (2018). De novo haplotype reconstruction in viral quasispecies using
491 paired-end read guided path finding. *Bioinformatics* 34, 2927-2935.
- 492 Chen, S., Zhou, Y., Chen, Y., and Gu, J. (2018). fastp: an ultra-fast all-in-one FASTQ preprocessor.
493 *Bioinformatics* 34, i884-i890.
- 494 Conceicao, C., Thakur, N., Human, S., Kelly, J.T., Logan, L., Bialy, D., Bhat, S., Stevenson-Leggett,
495 P., Zagrajek, A.K., Hollinghurst, P., *et al.* (2020). The SARS-CoV-2 Spike protein has a broad
496 tropism for mammalian ACE2 proteins. *PLoS Biol* 18, e3001016.
- 497 Corman, V.M., Muth, D., Niemeyer, D., and Drosten, C. (2018). Hosts and Sources of Endemic
498 Human Coronaviruses. *Adv Virus Res* 100, 163-188.
- 499 Fan, Y., Zhao, K., Shi, Z.L., and Zhou, P. (2019). Bat Coronaviruses in China. *Viruses* 11.

500 Forni, D., Cagliani, R., Clerici, M., and Sironi, M. (2017). Molecular Evolution of Human
501 Coronavirus Genomes. *Trends Microbiol* 25, 35-48.

502 Garry, R.F., Andersen, K.G., Gallaher, W.R., Lam T. T., Gangaparapu, K., Latif, A.A., Beddingfield,
503 B.J., Rambaut, A. and Holmes, E.C. (2021). Spike protein mutations in novel SARS-CoV-2 ‘variants
504 of concern’ commonly occur in or near indels, [https://virological.org/t/spike-protein-mutations-in-](https://virological.org/t/spike-protein-mutations-in-novel-sars-cov-2-variants-of-concern-commonly-occur-in-or-near-indels/605/1)
505 [novel-sars-cov-2-variants-of-concern-commonly-occur-in-or-near-indels/605/1](https://virological.org/t/spike-protein-mutations-in-novel-sars-cov-2-variants-of-concern-commonly-occur-in-or-near-indels/605/1).

506 Holmes, E.C., Andersen, K.G., Rambaut, A. and Garry, R.F. (2021). Spike protein sequences of
507 Cambodian, Thai and Japanese bat sarbecoviruses provide insights into the natural evolution of the
508 Receptor Binding Domain and S1/S2 cleavage site. [https://virological.org/t/spike-protein-](https://virological.org/t/spike-protein-sequences-of-cambodian-thai-and-japanese-bat-sarbecoviruses-provide-insights-into-the-natural-evolution-of-the-receptor-binding-domain-and-s1-s2-cleavage-site/622)
509 [sequences-of-cambodian-thai-and-japanese-bat-sarbecoviruses-provide-insights-into-the-natural-](https://virological.org/t/spike-protein-sequences-of-cambodian-thai-and-japanese-bat-sarbecoviruses-provide-insights-into-the-natural-evolution-of-the-receptor-binding-domain-and-s1-s2-cleavage-site/622)
510 [evolution-of-the-receptor-binding-domain-and-s1-s2-cleavage-site/622](https://virological.org/t/spike-protein-sequences-of-cambodian-thai-and-japanese-bat-sarbecoviruses-provide-insights-into-the-natural-evolution-of-the-receptor-binding-domain-and-s1-s2-cleavage-site/622).

511 Hu, B., Zeng, L.-P., Yang, X.-L., Ge, X.-Y., Zhang, W., Li, B., Xie, J.-Z., Shen, X.-R., Zhang, Y.-Z.,
512 Wang, N., et al. (2017). Discovery of a rich gene pool of bat SARS-related coronaviruses provides new
513 insights into the origin of SARS coronavirus. *PLoS pathogens* 13, p. e1006698.

514 Hughes, A. C., Satasook, C., Bates, P. J., Bumrungsri, S., & Jones, G. (2012). The projected effects
515 of climatic and vegetation changes on the distribution and diversity of Southeast Asian bats. *Global*
516 *Change Biology* 18, 1854-1865.

517 Vibol Hul, Deborah Delaune, Karlsson E.A., Hassanin A., Putita Ou Tey, Artem Baidaliuk, Fabiana
518 Gámbaro, Vuong Tan Tu, Lucy Keatts, Jonna Mazet, et al. (2021). A novel SARS-CoV-2 related
519 coronavirus in bats from Cambodia. bioRxiv, <https://doi.org/10.1101/2021.01.26.428212>.

520 Lam, T.T., Jia, N., Zhang, Y.W., Shum, M.H., Jiang, J.F., Zhu, H.C., Tong, Y.G., Shi, Y.X., Ni, X.B.,
521 Liao, Y.S., et al. (2020). Identifying SARS-CoV-2-related coronaviruses in Malayan pangolins.
522 *Nature* 583, 282-285.

523 Latinne, A., Hu, B., Olival, K.J., Zhu, G., Zhang, L., Li, H., Chmura, A.A., Field, H.E., Zambrana-
524 Torrelio, C., Epstein, J.H., et al. (2020). Origin and cross-species transmission of bat coronaviruses
525 in China. *Nat Commun* 11, 4235.

526 Letko, M., Seifert, S.N., Olival, K.J., Plowright, R.K., and Munster, V.J. (2020). Bat-borne virus
527 diversity, spillover and emergence. *Nat Rev Microbiol* 18, 461-471.

528 Li, D., Liu, C.M., Luo, R., Sadakane, K., and Lam, T.W. (2015). MEGAHIT: an ultra-fast single-node
529 solution for large and complex metagenomics assembly via succinct de Bruijn graph. *Bioinformatics* 31,

530 1674-1676.

531 Li, H., Handsaker, B., Wysoker, A., Fennell, T., Ruan, J., Homer, N., Marth, G., Abecasis, G., Durbin,
532 R., and Genome Project Data Processing, S. (2009). The Sequence Alignment/Map format and
533 SAMtools. *Bioinformatics* 25, 2078-2079.

534 Lole, K.S., Bollinger, R.C., Paranjape, R.S., Gadkari, D., Kulkarni, S.S., Novak, N.G., Ingersoll, R.,
535 Sheppard, H.W., and Ray, S.C. (1999). Full-length human immunodeficiency virus type 1 genomes
536 from subtype C-infected seroconverters in India, with evidence of intersubtype recombination. *J*
537 *Virology* 73, 152-160.

538 Lu, R., Zhao, X., Li, J., Niu, P., Yang, B., Wu, H., Wang, W., Song, H., Huang, B., Zhu, N., *et al.*
539 (2020). Genomic characterisation and epidemiology of 2019 novel coronavirus: implications for
540 virus origins and receptor binding. *Lancet* 395, 565-574.

541 Meleshko, D., Hajirasouliha, I., Korobeynikov, A. (2021). coronaSPAdes: from biosynthetic gene
542 clusters to RNA viral assemblies. bioRxiv, <https://doi.org/10.1101/2020.07.28.224584>.

543 Murakami, S., Kitamura, T., Suzuki, J., Sato, R., Aoi, T., Fujii, M., Matsugo, H., Kamiki, H., Ishida,
544 H., Takenaka-Uema, A., *et al.* (2020). Detection and Characterization of Bat Sarbecovirus
545 Phylogenetically Related to SARS-CoV-2, Japan. *Emerg Infect Dis* 26, 3025-3029.

546 Olival, K.J., Hosseini, P.R., Zambrana-Torrel, C., Ross, N., Bogich, T.L., and Daszak, P. (2017).
547 Host and viral traits predict zoonotic spillover from mammals. *Nature* 546, 646-650.

548 Sang, E.R., Tian, Y., Gong, Y., Miller, L.C., and Sang, Y. (2020). Integrate structural analysis,
549 isoform diversity, and interferon-inductive propensity of ACE2 to predict SARS-CoV2
550 susceptibility in vertebrates. *Heliyon* 6, e04818.

551 Sievers, F., Wilm, A., Dineen, D., Gibson, T.J., Karplus, K., Li, W., Lopez, R., McWilliam, H.,
552 Remmert, M., Soding, J., *et al.* (2011). Fast, scalable generation of high-quality protein multiple
553 sequence alignments using Clustal Omega. *Mol Syst Biol* 7, 539.

554 Stamatakis, A. (2014). RAxML version 8: a tool for phylogenetic analysis and post-analysis of large
555 phylogenies. *Bioinformatics* 30, 1312-1313.

556 Su, S., Wong, G., Shi, W., Liu, J., Lai, A.C.K., Zhou, J., Liu, W., Bi, Y., and Gao, G.F. (2016).
557 Epidemiology, Genetic Recombination, and Pathogenesis of Coronaviruses. *Trends Microbiol* 24,
558 490-502.

559 Wacharapluesadee, S., Tan, C.W., Maneerom, P., Duengkae, P., Zhu, F., Joyjinda, Y., Kaewpom, T.,

560 Chia, W.N., Ampoot, W., Lim, B.L., *et al.* (2021). Evidence for SARS-CoV-2 related coronaviruses
561 circulating in bats and pangolins in Southeast Asia. *Nat Commun* 12, 972.

562 Waterhouse, A., Bertoni, M., Bienert, S., Studer, G., Tauriello, G., Gumienny, R., Heer, F.T., de Beer,
563 T.A.P., Rempfer, C., Bordoli, L., *et al.* (2018). SWISS-MODEL: homology modelling of protein
564 structures and complexes. *Nucleic Acids Res* 46, W296-W303.

565 Wood, D.E., Lu, J., and Langmead, B. (2019). Improved metagenomic analysis with Kraken 2.
566 *Genome Biol* 20, 257.

567 Wu, F., Zhao, S., Yu, B., Chen, Y.M., Wang, W., Song, Z.G., Hu, Y., Tao, Z.W., Tian, J.H., Pei, Y.Y.,
568 *et al.* (2020a). A new coronavirus associated with human respiratory disease in China. *Nature* 579,
569 265-269.

570 Wu, L., Chen, Q., Liu, K., Wang, J., Han, P., Zhang, Y., Hu, Y., Meng, Y., Pan, X., Qiao, C., *et al.*
571 (2020b). Broad host range of SARS-CoV-2 and the molecular basis for SARS-CoV-2 binding to cat
572 ACE2. *Cell Discov* 6, 68.

573 Xiao, K., Zhai, J., Feng, Y., Zhou, N., Zhang, X., Zou, J.J., Li, N., Guo, Y., Li, X., Shen, X., *et al.*
574 (2020). Isolation of SARS-CoV-2-related coronavirus from Malayan pangolins. *Nature* 583, 286-
575 289.

576 Yan, H., Jiao, H., Liu, Q., Zhang, Z., Xiong, Q., Wang, B.J., Wang, X., Guo, M., Wang, L.F., Lan,
577 K., *et al.* (2021). ACE2 receptor usage reveals variation in susceptibility to SARS-CoV and SARS-
578 CoV-2 infection among bat species. *Nat Ecol Evol*.

579 Ye, Z.W., Yuan, S., Yuen, K.S., Fung, S.Y., Chan, C.P., and Jin, D.Y. (2020). Zoonotic origins of
580 human coronaviruses. *Int J Biol Sci* 16, 1686-1697.

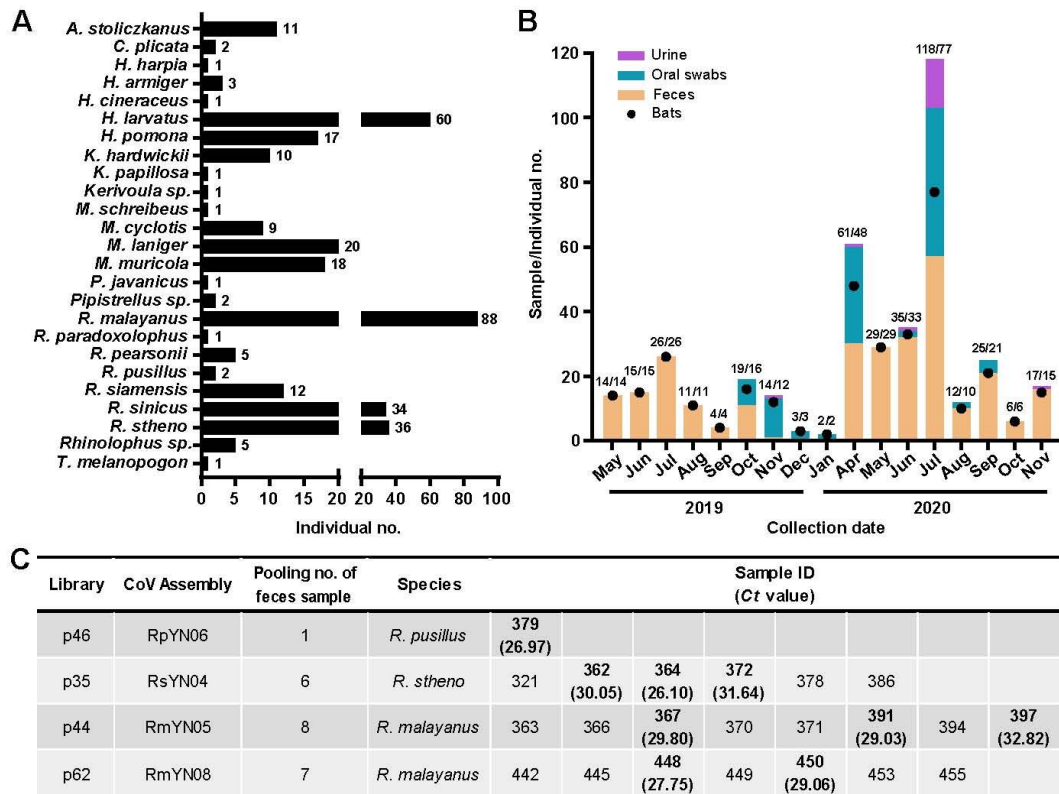
581 Zhou, H., Chen, X., Hu, T., Li, J., Song, H., Liu, Y., Wang, P., Liu, D., Yang, J., Holmes, E.C., *et al.*
582 (2020a). A Novel Bat Coronavirus Closely Related to SARS-CoV-2 Contains Natural Insertions at
583 the S1/S2 Cleavage Site of the Spike Protein. *Curr Biol* 30, 2196-2203 e2193.

584 Zhou, P., Fan, H., Lan, T., Yang, X.L., Shi, W.F., Zhang, W., Zhu, Y., Zhang, Y.W., Xie, Q.M., Mani,
585 S., *et al.* (2018). Fatal swine acute diarrhoea syndrome caused by an HKU2-related coronavirus of
586 bat origin. *Nature* 556, 255-258.

587 Zhou, P., Yang, X.L., Wang, X.G., Hu, B., Zhang, L., Zhang, W., Si, H.R., Zhu, Y., Li, B., Huang,
588 C.L., *et al.* (2020b). A pneumonia outbreak associated with a new coronavirus of probable bat origin.
589 *Nature* 579, 270-273.

590 Zhu, N., Zhang, D., Wang, W., Li, X., Yang, B., Song, J., Zhao, X., Huang, B., Shi, W., Lu, R., *et al.*
591 (2020). A Novel Coronavirus from Patients with Pneumonia in China, 2019. *N Engl J Med* 382,
592 727-733.
593

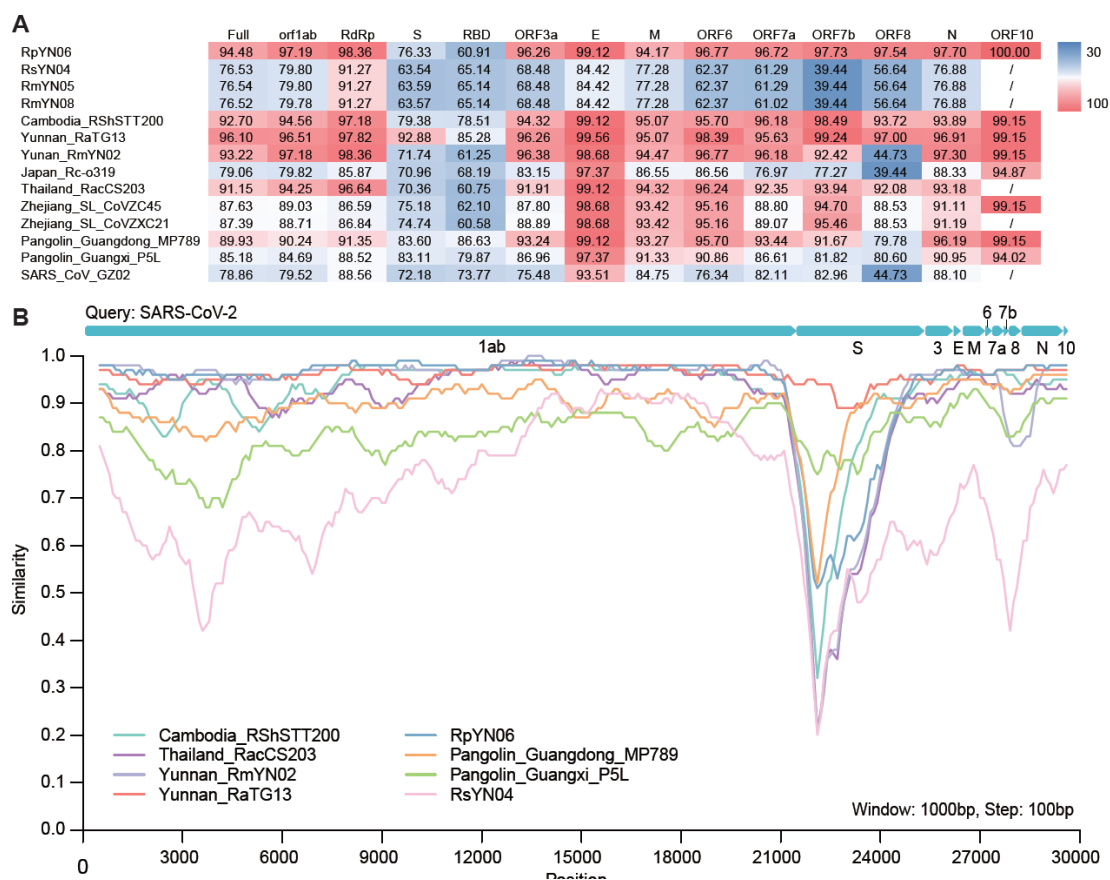
594 **Figure 1**



595

596

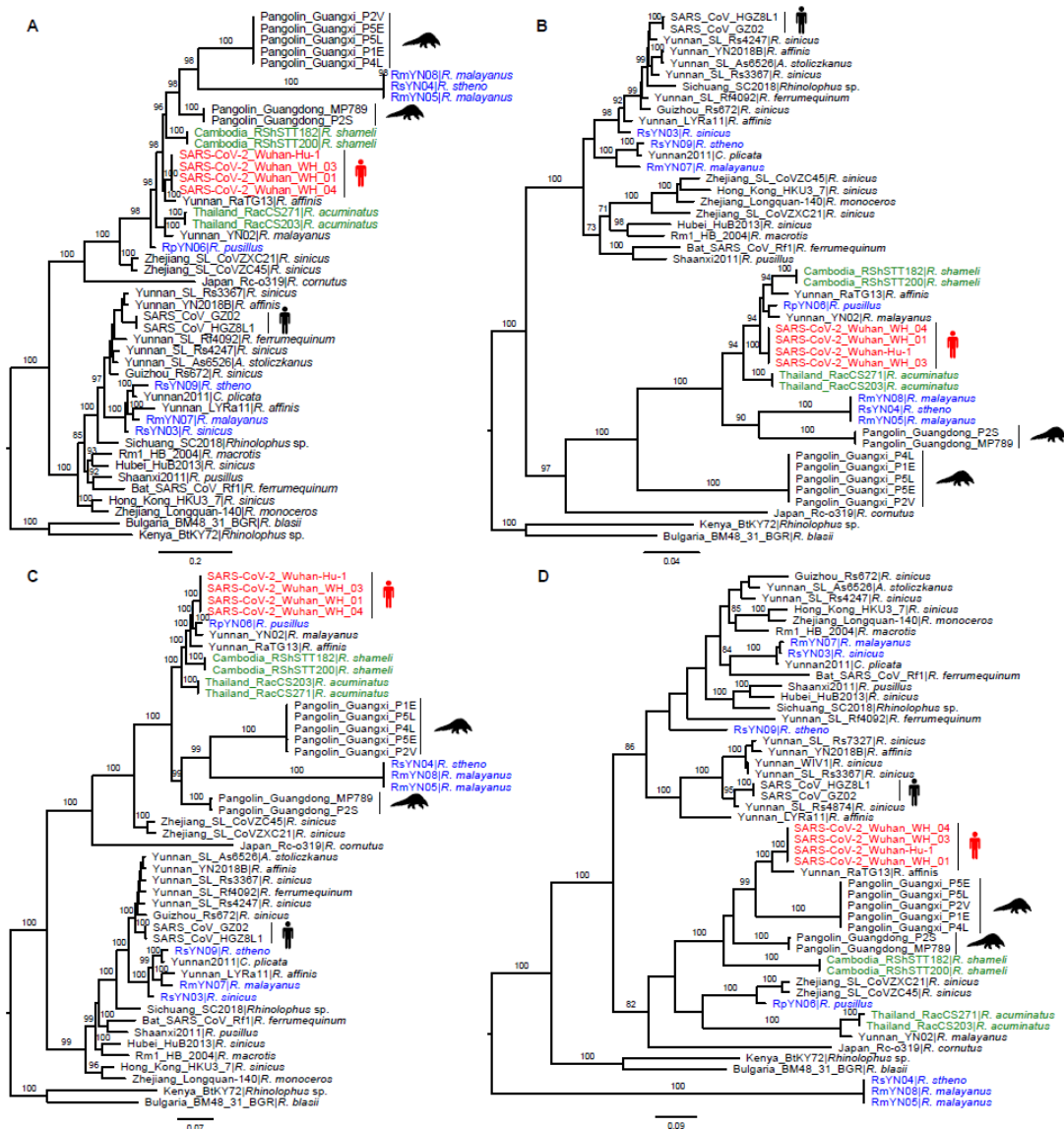
597 **Figure 2**



598

599

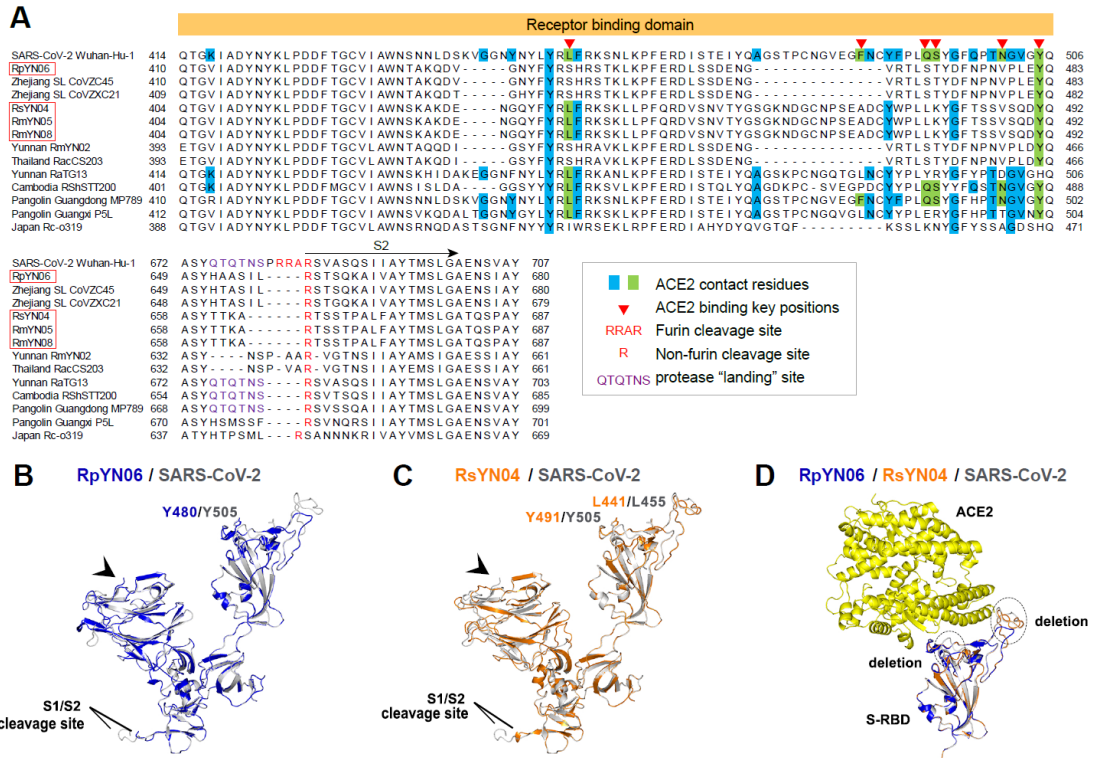
600 **Figure 3**



601

602

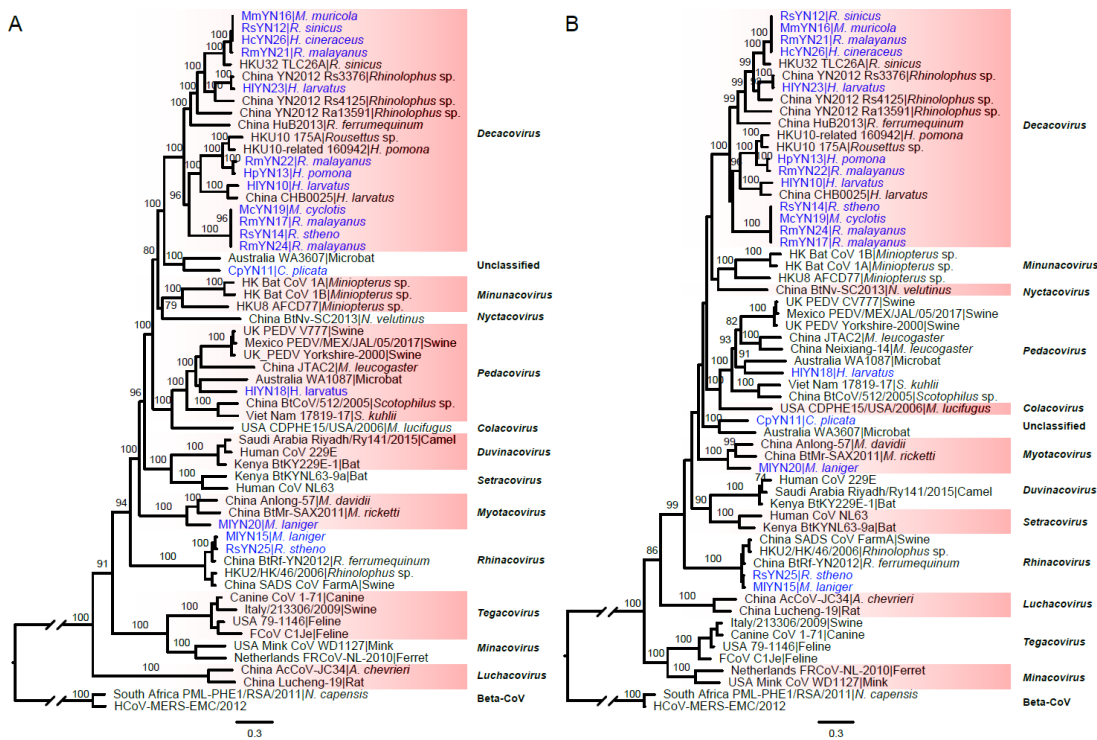
603 **Figure 4**



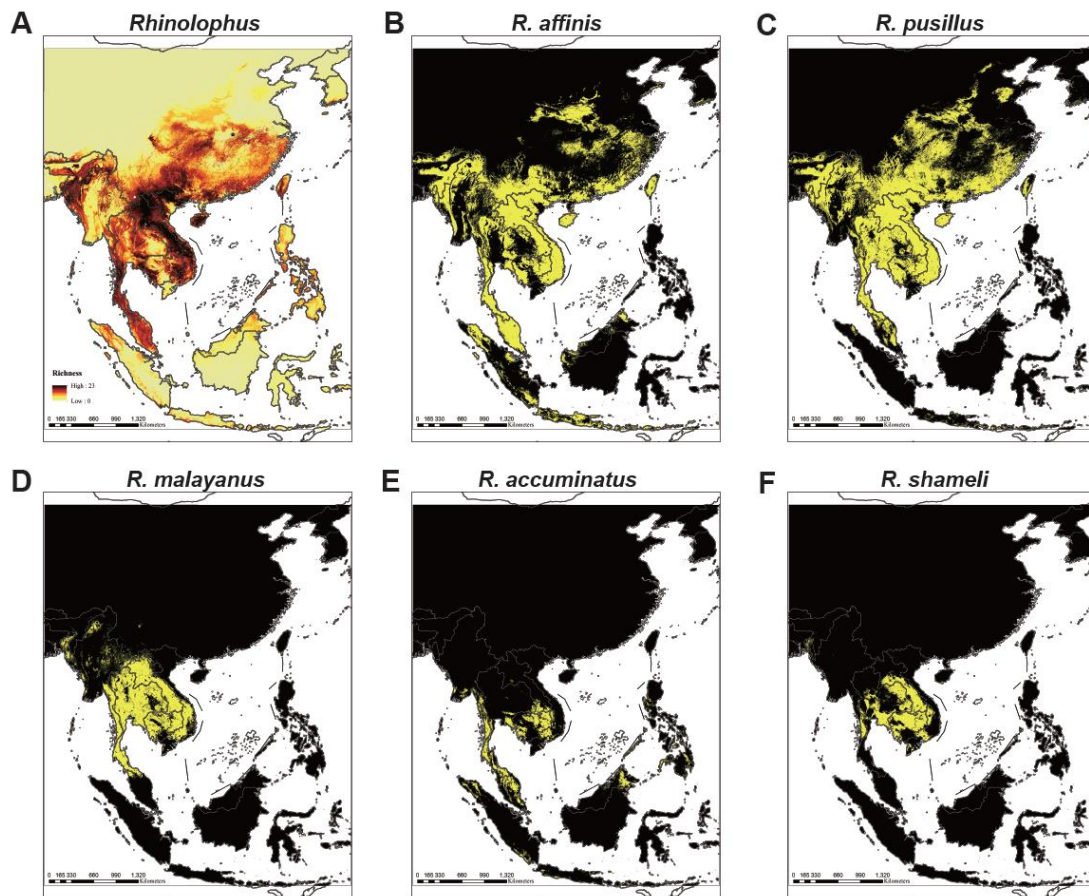
604

605

606 **Figure 5**



609 **Figure 6**



610

611 **STAR Methods**

612 **RESOURCE AVAILABILITY**

613 *Lead Contact*

614 Further information and requests for resources and reagents should be directed to and
615 will be fulfilled by the Lead Contact, Weifeng Shi (shiwf@ioz.ac.cn).

616 *Materials Availability*

617 This study did not generate new unique reagents.

618 **EXPERIMENTAL MODEL AND SUBJECT DETAILS**

619 A total of 23 different bat species were tested in this study (Table S1). Samples were
620 collected between May 2019 and November 2020 from Mengla County, Yunnan
621 Province in southern China (101.271563 E, 21.918897 N; 101.220091 E, 21.593202
622 N and 101.297471 E, 21.920934 N). The Xishuangbanna Tropical Botanical Garden
623 has an ethics committee that provided permission for trapping and bat surveys within
624 this study.

625 **METHOD DETAILS**

626 **Sample collection**

627 A total of 411 samples from 342 bats were collected from the Xishuangbanna Tropical
628 Botanical Garden and its adjacent areas, Mengla County, Yunnan Province in southern
629 China between May 2019 and November 2020. Bats were trapped using harp traps
630 and a variety of samples were collected from each individual bat including feces
631 (n=283), oral swab (n=109) and urine (n=19). Fecal and swab samples were collected
632 and stored in RNAlater (Invitrogen), and urine samples were directly collected in the
633 RNase-free tubes. These bats were primarily identified according to morphological
634 criteria and found to belong to 23 different species, with the majority representing

635 horseshoe bats (n=183) containing *Rhinolophus malayanus*, *R. stheno*, *R. sinicus*, *R.*
636 *siamensis*, *R. pusillus* and other *R.* genus bats, as well as *Hipposideros larvatus*
637 (n=59) (Table S1). All bats were sampled alive and subsequently released. All samples
638 were transported on ice and then kept at -80°C until use.

639 **Next generation sequencing**

640 All bat samples were merged into 100 pools to generate sequencing libraries, based on
641 the sample types, bat species and collection date. Of these bat libraries, 18 libraries
642 have been described previously (Zhou et al., 2020a), including the library from which
643 the viruses RmYN01 and RmYN02 were identified. These 18 libraries were combined
644 with 82 additional libraries newly obtained here. Total RNA from samples was
645 extracted using RNAPrep pure Cell/Bacteria Kit (TianGen) and aliquots of the RNA
646 solutions were then pooled in equal volume. Libraries were constructed using the
647 NEBNext Ultra Directional RNA Library Prep Kit for Illumina (NEB). Ribosomal (r)
648 RNA of fecal, oral swab and urine was removed using the TransNGS rRNA Depletion
649 (Bacteria) Kit (TransGen) and rRNA of tissues was removed using TransNGS rRNA
650 Depletion (Human/Mouse/Rat) Kit (TransGen), respectively. Paired-end (150 bp)
651 sequencing of each RNA library was performed on the NovaSeq 6000 platform
652 (Illumina) with the S4 Reagent Kit, and performed by the Novogene Bioinformatics
653 Technology (Beijing, China).

654 **Genome assembly and annotation**

655 Clean reads from the next generation sequencing were classified with Kraken (v2.0.9)
656 based on all microbial sequences from the NCBI nucleotide database. Paired-end
657 reads classified as from coronaviruses were extracted from the Kraken output. To
658 further verify the existence of coronaviruses, reads classified as coronaviruses were
659 assembled with MEGAHIT (v1.2.9). The contigs from MEGAHIT were searched by
660 BLASTn based on the NCBI nt database. Sequencing libraries with contigs identified
661 as representing coronavirus were *de novo* assembled with coronaSPAdes (v3.15.0).
662 The near complete genomes of coronavirus were then identified from the results of
663 coronaSPAdes by BLASTn searching.

664 The newly assembled coronavirus genomes were validated by read mapping using
665 Bowtie2 (v2.4.1). The coverage and depth of coronavirus genomes were calculated
666 with SAMtools (v1.10) based on SAM files from Bowtie2. To further improve the
667 quality of the genome annotations, SAM files of the reads mapping to SARS-CoV-2
668 were checked manually with Geneious (v2021.0.1), extending the ends as much as
669 possible. The open reading frames (ORFs) of the verified genome sequences were
670 annotated using Geneious (v2021.0.1) and then checked with closed references from
671 NCBI. The taxonomy of these newly assembled coronavirus genome were determined
672 by online BLAST (<https://blast.ncbi.nlm.nih.gov/Blast.cgi>).

673 Coronavirus contigs produced by MEGAHIT (v1.2.9) were analyzed to evaluate the
674 existence of coronavirus sequences in each library. To mitigate the possibility of false
675 positives due to index hopping, coronavirus contigs from different libraries within the
676 same chip and same lane were compared, and if a shorter contig shared >99%
677 nucleotide sequence identity with a longer contig from another library, the shorter one
678 was removed.

679 **Sanger sequencing**

680 The assembled genome sequences of the beta-CoVs identified here were further
681 confirmed by quantitative real-time PCR (qPCR), PCR amplification and Sanger
682 sequencing. A TaqMan-based qPCR was first performed to test the feces of pools p19,
683 p35, p44, p46, p52 and p62, as these contained beta-CoVs according to the
684 metagenomic analysis. cDNA synthesis was performed using the ReverTra Ace qPCR
685 RT Kit (TOYOBO). The qPCR reaction was undertaken using a set of probe and
686 primer pairs (Table S4) in the *Pro Taq* HS Premix Probe qPCR Kit (AG) with a
687 LightCycler 96 Real-Time PCR System (Roche).

688 ***Rapid amplification of cDNA ends (RACE)***. The sequences of the 5' and 3' termini
689 were obtained by RACE using the SMARTer RACE 5'/3' Kit and 3'-Full RACE Core
690 Set (Takara), according to the manufacturer's instructions with some minor
691 modifications. Two sets of gene-specific primers (GSPs) and nested-GSPs (NGSPs)
692 for 5' and one set for 3' RACE PCR amplification were designed based on the

693 assembled genome sequences of six beta-CoVs (Table S3). The first round of
694 amplification was performed by touchdown PCR, while the second round comprised
695 regular PCR. The PCR amplicons of ~1000 bp fragments of the two regions were
696 obtained separately and sequenced with the amplified primer or gel purified followed
697 by ligation with the pMD18-T Simple Vector (TaKaRa) and transformation into
698 competent *Escherichia coli* DH5 α (Takara). Insertion products were sequenced with
699 M13 forward and reverse primers.

700 ***Amplification of beta-CoVs S gene and the host COI gene.*** Based on the spike gene
701 and the adjacent sequences of RsYN04, RmYN05, RmYN08 and RpYN06, 9 primer
702 pairs were designed for Sanger sequencing (Table S4). The cDNAs reverse
703 transcribed above were used as templates. The thermal cycling parameters of PCR
704 amplification were as follows: 5 mins at 95°C; followed by 30 s at 95°C, 30 s at 50°C
705 (an exception of 55°C for primers 379SF5/379SR5), 1 min at 72°C for 30 cycles; and
706 10 min at 72°C. A second round PCR was then performed under the same conditions
707 with the corresponding PCR products used as templates. Further confirmation of host
708 species was based on analysis of the cytochrome b (*cytb*) gene obtained from the
709 assembled contigs. We also amplified and sequenced the fragment of cytochrome c
710 oxidase subunit I (*COI*) gene using primers VF1/VR1 (Ivanova et al., 2007). Briefly,
711 the following touchdown PCR conditions were used: 30 s at 95°C, 30 s at 52°C to
712 45°C, 45 s at 72°C for 14 cycles; and followed by 30 s at 95°C, 30 s at 45°C, 45 s at
713 72°C for 30 cycles.

714 **Bioinformatics analyses**

715 ***Phylogenetic analysis.*** Multiple sequence alignment of the alphacoronavirus and
716 betacoronavirus nucleotide sequences was performed using MAFFT (v7.450).
717 Phylogenetic analysis of the complete genome and major genes were performed using
718 the maximum likelihood (ML) method available in RAxML (v8.2.11) with 1000
719 bootstrap replicates, employing the GTR nucleotide substitution model and a gamma
720 distribution of rate variation among sites. The resulting phylogenetic trees were
721 visualized using Figtree (v1.4.4).

722 ***Sequence identity and recombination analysis.*** Pairwise sequence identity of the
723 complete viral genome and genes between SARS-CoV-2 and representative
724 sarbecoviruses was calculated using Geneious (v2021.0.1). A whole genome sequence
725 similarity plot was performed using Simplot (v3.5.1), with a window size of 1000bp
726 and a step size of 100bp.

727 ***Site and structural analysis of the spike gene.*** The three-dimensional structures of
728 the S1 protein from RpYN06, RsYN04 and SARS-CoV-2 were modeled using the
729 Swiss-Model program (Waterhouse et al., 2018) employing PDB: 7A94.1 as the
730 template. Molecular images were generated with an open-source program - PyMOL.
731 Multiple sequence alignment of spike gene amino acid sequences was performed with
732 Clustal Omega (v1.2.2).

733 **Ecological modeling**

734 Data was collated using a combination of that from Hughes 2019, from various online
735 repositories (Table S7), and additional GBIF data collated between 2017 and 2021.
736 Further data was downloaded for Indonesia since 1990, even though wide-scale
737 deforestation means that most species are to still likely to occupy small parts of their
738 range. This provided sufficient data to model 49 Rhinolophid species based on 8418
739 occurrence points (once any duplicate points of species recorded repeatedly at the
740 same location had been removed), with almost all records collected since 1998.
741 Variables were selected to provide a good simulation of the environmental conditions
742 that may shape species distributions, whilst minimizing the number of variables to
743 allow modelling of species with few occurrence records. Variables included a number
744 of bioclimatic parameters (1,2,4,5,11,12,13,14,15 : <http://worldclim.org/version2>) in
745 addition to productivity and other climate metrics (NDVI, seasonality, actual
746 evapotranspiration, potential evapotranspiration seasonality and mean annual potential
747 evapotranspiration, aridity, Emberger's pluviotonic quotient, continentality,
748 thermicity, maximum temperature of the coldest month - <http://envirem.github.io/>) -
749 and both NDVI seasonality and mean). In addition, we included some topographic
750 variables including soil pH, distance to bedrock, average tree height and tree density.

751 All variables were clipped to a mask of Tropical Southeast Asia and southern China at
752 a resolution of 0.008 decimal degrees (approximately 1km²) in ArcMap 10.3, then
753 converted to ascii format for modelling.

754 Models of Rhinolophid diversity were run in Maxent 3.4.4. Five replicates were run
755 for each species, and the average taken before reclassifying with the 10th percentile
756 cumulative logistic threshold to form binary maps for each species (see Hughes et al.,
757 2013). AUC for training and testing was 0.96 and 0.92 respectively, and all training
758 AUCs were above 0.88.

759 Because of complex regional biogeography, optimal species habitat can exist in areas
760 that have not been colonized. Therefore, we downloaded mapped ranges for 39 of the
761 49 species modelled from the IUCN ([https://www.iucnredlist.org/resources/spatial-](https://www.iucnredlist.org/resources/spatial-data-download)
762 [data-download](https://www.iucnredlist.org/resources/spatial-data-download)). Bats were extracted from this data, clipped to match the study area.

763 We then divided the IUCN data into five regions; mainland Southeast Asia,
764 Philippines, Java-Sumatra, Borneo and Sulawesi-Moluccas, using shapefiles of each
765 region to clip out bats listed there. This was collated to form a spreadsheet listing each
766 zone each species was listed in, and then the appropriate shapefiles used to determine
767 the ranges of each species (although only 39 of the 49 species could be treated in this
768 way). Each species was then remosaiced with the mask to provide a binary
769 distribution map, removing any potentially suitable areas that were outside the species
770 biogeographic range. Stricter filters were not used, because for the majority of species
771 there is not a clear analysis of genuine delineations of species ranges of if these
772 species are migratory. These binary mosaicked maps were then summed with the
773 other ten species using the mosaic tool to generate a map of richness for the region.

774 **QUANTIFICATION AND STATISTICAL ANALYSIS**

775 No statistical analyses were conducted as part of this study.